



HAL
open science

A Compound Polarimetric-Textural Approach for Unsupervised Change Detection in Multi-Temporal Full-Pol SAR Imagery

Davide Pirrone, Minh-Tan Pham

► **To cite this version:**

Davide Pirrone, Minh-Tan Pham. A Compound Polarimetric-Textural Approach for Unsupervised Change Detection in Multi-Temporal Full-Pol SAR Imagery. 2020 IEEE International Geoscience and Remote Sensing Symposium (IGARSS 2020), IEEE, Sep 2020, Waikoloa, HI (virtual), United States. 10.1109/IGARSS39084.2020.9323565 . hal-03934112

HAL Id: hal-03934112

<https://hal.science/hal-03934112>

Submitted on 11 Jan 2023

HAL is a multi-disciplinary open access archive for the deposit and dissemination of scientific research documents, whether they are published or not. The documents may come from teaching and research institutions in France or abroad, or from public or private research centers.

L'archive ouverte pluridisciplinaire **HAL**, est destinée au dépôt et à la diffusion de documents scientifiques de niveau recherche, publiés ou non, émanant des établissements d'enseignement et de recherche français ou étrangers, des laboratoires publics ou privés.

A COMPOUND POLARIMETRIC-TEXTURAL APPROACH FOR UNSUPERVISED CHANGE DETECTION IN MULTI-TEMPORAL FULL-POL SAR IMAGERY

*Davide Pirrone**, *Minh-Tan Pham†*

* LISTIC - Université Savoie Mont Blanc, F-74000 Annecy, France. E-mail: davide.pirrone@alumni.unitn.it

† IRISA - Université Bretagne-Sud, UMR 6074, 56000 Vannes, France. E-mail: minh-tan.pham@irisa.fr

ABSTRACT

Change Detection represents a relevant topic for the analysis of multi-temporal analysis of Polarimetric SAR (PolSAR) data. However, most of the CD approaches for PolSAR imagery do not take into account textural information, which can be useful for have larger performance robustness. In this work, we propose a novel approach for unsupervised change detection considering polarimetric and textural information from multi-temporal PolSAR imagery. The approach is based on the joint use of features from coherency matrix and gradient tensor and the definition of a multi-temporal distance. A binary unsupervised thresholding is used for discriminating change and no-change classes. Experimental results obtained on a multi-temporal PolSAR dataset over Los Angeles area illustrate the effectiveness of the proposed approach.

Index Terms— Polarimetric SAR, change detection, gradient tensor, unsupervised detection

1. INTRODUCTION

Multi-temporal environmental monitoring plays an important role in remote sensing, with different applications associated both to natural and urban scenes [1]. This makes Change Detection (CD) one of the hot topics for the remote sensing imagery. In particular, the large amount of data available from satellite and airborne sensors drives the research towards the development of automatic CD strategies.

Polarimetric SAR (PolSAR) represents one of the most interesting sensors for CD applications, as it is a microwave active system that guarantees acquisitions for all light and weather conditions with large scattering information. A large effort in the literature has been devoted to the development of classification techniques based on PolSAR imagery [2]. A smaller effort has been spent in the development of PolSAR-based CD strategies, based on the scattering information of the single pixel. These are typically based on the definition of the log-likelihood ratio [3], statistical modeling [4] or polarimetric distance measures [5, 6]. However, texture represents an additional information source for target discrimination in SAR imagery. Some of state-of-the-art texture-based classification approaches considers the combination of

the radiometric information with textures from Gray Level Co-occurrence Matrix (GLCM) [7], Gabor filters [8] or gradient tensors [9, 10]. To the best of our knowledge, a very small effort has been spent in combining radiometric and textural information for CD in PolSAR data. In this work, we present a novel CD approach from multi-temporal PolSAR images. The approach considers a weighted multi-looking of the coherency information in both pre- and post-event. Next, a feature vector for the two images is built by considering both the radiometric and the textural information. The radiometric information is given by the multi-looked terms of the covariance matrix. The textural information is given by the gradient tensors of the covariance matrix, extracted based on the min-ratio operator along multiple directions [10]. A statistical distance between the two feature vectors is defined as a Change Index (CI) and thresholded.

The reminder of this paper is organized as follows. Section 2 describes the proposed methodology for the PolSAR based change detection. Section 3 provides some experimental results on a full-pol dataset from UAVSAR sensor. Section 4 presents the conclusions and possible future developments of the proposed work.

2. METHODOLOGY

Let us consider two images from PolSAR sensor acquired on two times $t_1, t_2, t_1 < t_2$, respectively. The proposed approach aims at identifying the set of changed and unchanged pixels, associated to classes ω_c, ω_u , respectively. Fig. 1 shows the block scheme for the proposed approach. Four main stages are composing the scheme, namely: i) generation of the multi-look Coherency matrix for single-time images; ii) generation of the texture descriptors for the single-time images, based on the De Zenzo gradient tensor [10]; iii) definition of the CI feature; iv) thresholding and generation of the CD map.

2.1. Estimation of multi-look weighted coherency

Let us consider a PolSAR image acquired at time $t_i, i = 1, 2$. PolSAR measures complex scattering by transmitting and/or receiving radiation on multiple polarizations (e.g., H and V

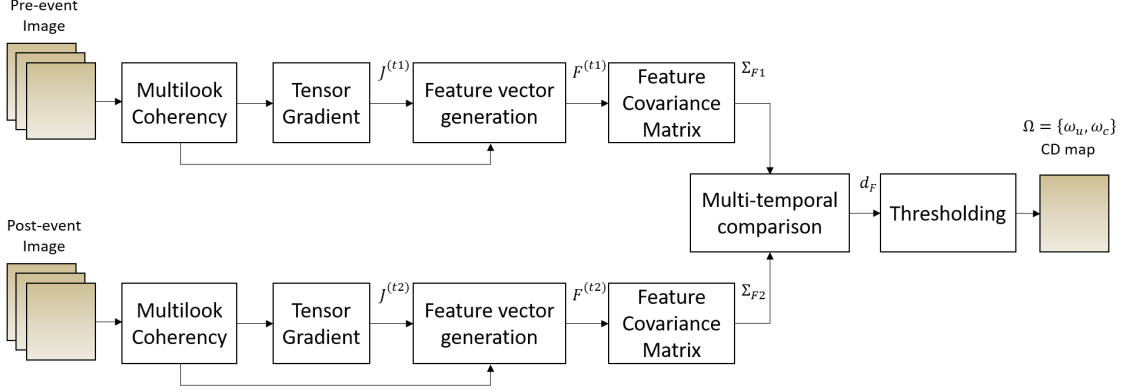


Fig. 1: Block scheme for the proposed approach.

linear polarizations). The complex information can be represented, under the Pauli basis, in form of a scattering vector $k_p = [S_{hh}]$, being the S_{pq} the complex scattering coefficient measured transmitting on polarization q and receiving on polarization q [11]. The scattering vector is a proper descriptor for coherent targets, but it fails in presence of distributed targets, where the scattering of each cell is composed by terms associated to multiple scatterers. In this case, the scattering information is described by a second-order statistics as the hermitian Coherency matrix T .

$$T = \frac{1}{L} \sum_L k_p k_p^H = \begin{bmatrix} T_{11} & T_{12} & T_{13} \\ T_{21} & T_{22} & T_{23} \\ T_{31} & T_{32} & T_{33} \end{bmatrix} \quad (1)$$

being $k_p = \frac{1}{\sqrt{(2)}} [S_{HH} + S_{VV}; S_{HH} - S_{VV}; 2S_{HV}]$ the scattering vector in the Pauli basis and $(\cdot)^H$ the hermitian operator.

2.2. Texture description based on gradient tensor

Texture information can be often considered as a precious support for making image analysis more robust by taking into account neighborhood information. In the literature, several texture descriptors have been defined, in terms of transform domain [12], image statistics [13] or GLCM [7]. In this work, a gradient tensor measure is selected as texture descriptor for multi-channel data, thanks to its small computational cost and the possibility to extract inter-channel correlation information on the gradient coefficients. Let I be a data-cube containing the independent elements of the T hermitian matrix.

$$I = [|T_{11}|, |T_{12}|, |T_{13}|, |T_{22}|, |T_{23}|, |T_{33}|] \quad (2)$$

Let I_i be the i -th channel of I . For each position (x, y) , spatial derivatives of I along x - and y -axis, namely I_{ix} and I_{iy} , are derived. From the derivatives, a gradient tensor J is obtained by summing the derivative information along the different im-

age channels.

$$J = \begin{bmatrix} \sum_{i=1}^6 (I_{ix})^2 & \sum_{i=1}^6 I_{ix} I_{iy} \\ \sum_{i=1}^6 I_{ix} I_{iy} & \sum_{i=1}^6 (I_{iy})^2 \end{bmatrix} = \begin{bmatrix} J_{11} & J_{12} \\ J_{21} & J_{22} \end{bmatrix} \quad (3)$$

Because of the SAR image statistics, a min-ratio operator is considered for computing the spatial derivatives with respect to pixel neighborhood.

$$I_{ix}(x, y) = 1 - \min \left\{ \frac{I_i(x+1, y)}{I_i(x-1, y)}, \frac{I_i(x-1, y)}{I_i(x+1, y)} \right\} \quad (4)$$

$$I_{iy}(x, y) = 1 - \min \left\{ \frac{I_i(x+1, y)}{I_i(x, y-1)}, \frac{I_i(x, y-1)}{I_i(x, y+1)} \right\} \quad (5)$$

2.3. Generation of the combined change index

Based on the texture-based global information in J and polarimetric pixel-based information in T , a feature vector F is constructed. In order to reduce the dimensionality of the vector, while keeping most of the information, just diagonal elements from T are considered.

$$F = \left[\sqrt{|T_{11}|}, \sqrt{|T_{22}|}, \sqrt{|T_{33}|}, |J_{11}|, |J_{12}|, |J_{22}| \right] \quad (6)$$

In order to consider the local dispersion of the vector F , covariance matrix C_F is considered. This is estimated on a moving square window around pixel (x, y) , as follows:

$$\Sigma_F(x, y) = \frac{1}{K-1} \sum_{i \in N_i} (F_i - \mu_F)^T (F_i - \mu_F) \quad (7)$$

being $\mu_F = \frac{1}{K-1} \sum_{i \in N_i} F_i$ the vector mean.

Let Σ_{F1}, Σ_{F2} be feature covariance matrices obtained at times t_1, t_2 , derived from vectors $F^{(t1)}, F^{(t2)}$, respectively. A multi-temporal compound change index d_F is defined as log-euclidean distance of the two single-time vectors.

$$d_F = \|\log(C_{F2}) - \log(C_{F1})\|_F \quad (8)$$

On one hand, d_F shows high values in presence of changes, because of the large distances between the two covariance matrices. On the other hand, it shows values close to zero for unchanged targets.

2.4. CI thresholding and generation of the CD map

An unsupervised strategy for the detection of changed areas is applied on d_F , considering the binary problem with classes ω_u, ω_c . In particular, Otsu thresholding is considered as thresholding strategy. For binary Otsu thresholding, the probability density function of d_F can be modeled as a mixture of two components:

$$P(d_F) = P(\omega_u)p(d_F|\omega_u) + P(\omega_c)p(d_F|\omega_c) \quad (9)$$

being $P(\omega), p(d_F|\omega)$ the prior probability and the marginal distribution for the class $\omega, \omega \in \{\omega_u, \omega_c\}$. An optimal threshold d_{FT} is selected by minimizing the weighted sum of class variance for the two classes $var(\omega_u), var(\omega_c)$.

$$d_F = \arg \min_{d_F} [P(\omega_u)var(\omega_u) + P(\omega_c)var(\omega_c)] \quad (10)$$

3. EXPERIMENTAL RESULTS

A validation campaign for the proposed approach has been conducted with a full-polarimetric multi-temporal dataset acquired by UAVSAR mission over Los Angeles, California (U.S.A.). The two images, acquired in 2009 (see Fig. 2-a) and 2015 (see Fig. 2-b), have size 559×400 pixels and show changes due to urbanization phenomenon, with the creation of new urban areas and the removal of vegetated areas for future built-up areas. The two images have been both acquired with a spatial resolution of 0.4×1.6 meters and pre-processed with calibration and co-registration. Fig. 2-c shows the reference map obtained by photo-interpretation of the Pauli RGB of the single-time PolSAR images. The proposed approach has been compared with other state-of-the-art CD techniques based on full-polarimetric imagery. In particular, several techniques were considered, namely a Log-Likelihood Ratio (LLR) test [3], the Hotelling-Lawley trace (HLT) [14] and PCA-based K-means based of geodesic distance measure (GD-PCAK) [5]. For all the approaches, performance has been evaluated in terms of overall accuracy OA and Cohen's coefficient $Kappa$.

For both single-time images, coherency matrix has been generated, resulting in a final multi-looking resolution of 3×3 meters. Gradient tensor has been computed and diagonal components have been used to create the vectors $F^{(t1)}, F^{(t2)}$. Feature covariance matrices Σ_{F1}, Σ_{F2} have been derived by considering a local neighborhood of 7×7 pixels. Fig. 3-a shows the output CD map. Good detection performance can be inferred from its comparison with the reference map. In particular, a good tradeoff in terms of detail preservation and homogeneity for the changed regions is inferred. This resulted in numerical values $OA = 0.9728$ and $Kappa = 0.7133$ (see Table 1). Table 2 illustrates the performance comparison of the proposed approach with respect to the literature. The proposed approach shows an increment of 0.5% for OA and 21% for $Kappa$ with respect to LLR approach (see

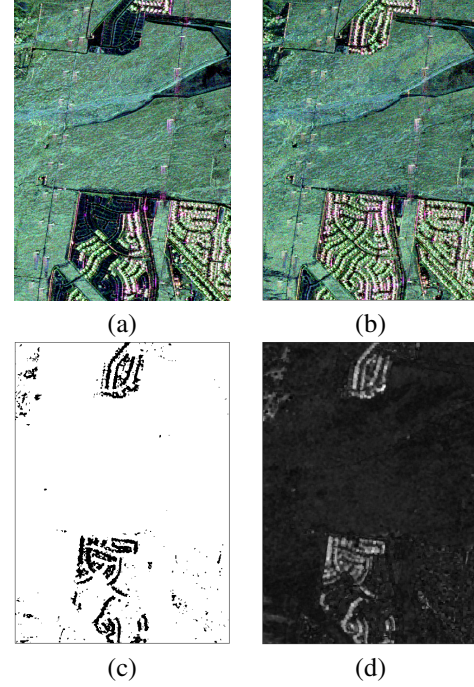


Fig. 2: Pauli RGB for (a) pre-event and (b) post-event image; (c) reference map; (d) log-euclidean distance d_F .

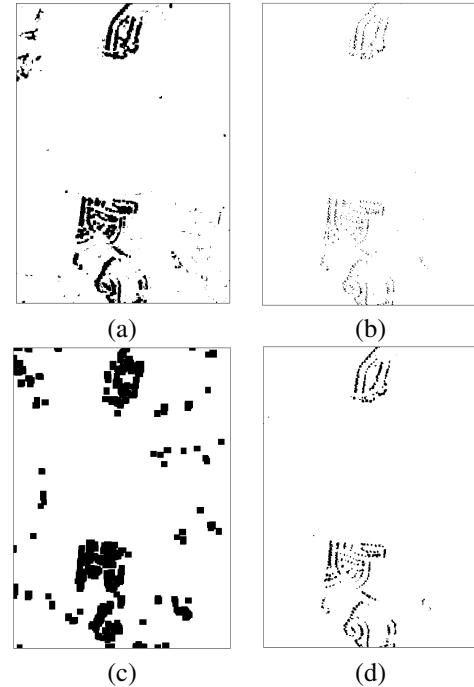


Fig. 3: CD Map using: (a) proposed approach; (b) HLT; (c) GD-PCAK; (d) LLR.

Fig. 3-d). Larger improvements are registered with respect to the HLT (see Fig. 3-b) and the GD-PCAK (see Fig. 3-c).

Table 1: Confusion Matrix for the proposed approach.

	$\hat{\omega}_u$	$\hat{\omega}_c$
ω_u	209403	3082
ω_c	2997	8118
	OA	0.9728
	Kappa	0.7133

Table 2: Overview of Performance assessment.

Method	OA	Kappa
Proposed	0.9728	0.7133
HLT	0.9564	0.2112
LLR	0.9673	0.4989
GD-PCAK	0.9115	0.4067

4. CONCLUSIONS

In this work, a novel CD approach for multi-temporal PolSAR images has been presented. The method considers the use of overall gradient tensor information from multiple polarimetric channels. A multi-temporal distance measure is based on compound textural-polarimetric features from the single-time matrices and thresholded for obtaining the final CD map. Preliminary experimental results show good detection capabilities, with performance larger than other literature techniques. Future developments aim at analyzing the distance measure based on the PolSAR image statistics and integrating advanced polarimetric features in the approach.

5. REFERENCES

- [1] F. Bovolo and L. Bruzzone, "The time variable in data fusion: A change detection perspective," *IEEE Geoscience and Remote Sensing Magazine*, vol. 3, pp. 8–26, 2015.
- [2] V. Alberga, "A study of land cover classification using polarimetric sar parameters," *International Journal of Remote Sensing*, vol. 28, no. 17, pp. 3851–3870, 2007.
- [3] K. Conradsen, A. A. Nielsen, J. Schou, and H. Skriver, "A test statistic in the complex wishart distribution and its application to change detection in polarimetric sar data," *IEEE Transactions on Geoscience and Remote Sensing*, vol. 41, no. 1, pp. 4–19, 2003.
- [4] M. Liu, H. Zhang, C. Wang, and F. Wu, "Change detection of multilook polarimetric sar images using heterogeneous clutter models," *IEEE Transactions on Geoscience and Remote Sensing*, vol. 52, no. 12, pp. 7483–7494, 2014.
- [5] D. Ratha, S. De, T. Celik, and A. Bhattacharya, "Change detection in polarimetric sar images using a geodesic distance between scattering mechanisms," *IEEE Geoscience and Remote Sensing Letters*, vol. 14, no. 7, pp. 1066–1070, 2017.
- [6] D. Pirrone, F. Bovolo, and L. Bruzzone, "A novel framework for change detection in bi-temporal polarimetric sar images," in *Image and Signal Processing for Remote Sensing XXII*, vol. 10004, p. 100040Z, International Society for Optics and Photonics, 2016.
- [7] M. Kuffer, K. Pfeffer, R. Sliuzas, and I. Baud, "Extraction of slum areas from vhr imagery using glm variance," *IEEE Journal of selected topics in applied earth observations and remote sensing*, vol. 9, no. 5, pp. 1830–1840, 2016.
- [8] H.-C. Li, T. Celik, N. Longbotham, and W. J. Emery, "Gabor feature based unsupervised change detection of multitemporal sar images based on two-level clustering," *IEEE Geoscience and Remote Sensing Letters*, vol. 12, no. 12, pp. 2458–2462, 2015.
- [9] M.-T. Pham, G. Mercier, and J. Michel, "Covariance-based texture description from weighted coherency matrix and gradient tensors for polarimetric sar image classification," in *Geoscience and Remote Sensing Symposium (IGARSS), 2015 IEEE International*, pp. 2469–2472, IEEE, 2015.
- [10] M.-T. Pham, "Fusion of polarimetric features and structural gradient tensors for vhr polsar image classification," *IEEE Journal of Selected Topics in Applied Earth Observations and Remote Sensing*, vol. 11, no. 10, pp. 3732–3742, 2018.
- [11] J. Lee and E. Pottier, *Polarimetric Radar Imaging: From Basics to Applications*. Optical Science and Engineering, Taylor & Francis, 2009.
- [12] B. Brisco, A. Schmitt, K. Murnaghan, S. Kaya, and A. Roth, "Sar polarimetric change detection for flooded vegetation," *International Journal of Digital Earth*, vol. 6, no. 2, pp. 103–114, 2013.
- [13] X. Deng and C. López-Martínez, "Higher order statistics for texture analysis and physical interpretation of polarimetric sar data," *IEEE Geoscience and Remote Sensing Letters*, vol. 13, no. 7, pp. 912–916, 2016.
- [14] V. Akbari, S. N. Anfinson, A. P. Doulgeris, T. Eltoft, G. Moser, and S. B. Serpico, "Polarimetric sar change detection with the complex hotelling–lawley trace statistic," *IEEE Transactions on Geoscience and Remote Sensing*, vol. 54, no. 7, pp. 3953–3966, 2016.